

1
2
3
4
5
6
7
8
9
10
11
12
13
14
15
16
17
18
19
20
21

Retinal and post-retinal contributions to the Quantum efficiency of the human eye.

Authors: Gibran Manasseh^{1*}, Chloe de Balthasar¹, Bruno Sanguinetti², Enrico Pomarico², Nicolas Gisin², Rolando Grave de Peralta¹, Sara L. Gonzalez¹

¹Electrical Neuroimaging Group, Department of Clinical Neuroscience, Faculty of Medicine, Switzerland

²Group of Applied Physics, Faculty of Physics, University of Geneva, Switzerland

Correspondence :
Gibran Manasseh
University of Geneva
Department of Clinical Neuroscience
Faculty of Medicine
Rue Gabrielle-Perret-Gentil, 4
1211 Geneva 14
Switzerland

Keywords: quantum efficiency, photons, human vision, retina, dim light, scotopic vision, reaction time, EEG

22 Abstract: The retina is one of the best known quantum detectors with rods
23 able to respond to a single photon. However, estimates on the number of photons
24 eliciting conscious perception, based on signal detection theory, are
25 systematically above these values. One possibility is that post-retinal processing
26 significantly contributes to the decrease in the quantum efficiency determined by
27 signal detection. We carried out experiments in humans using controlled sources
28 of light while recording EEG and reaction times. Half of the participants behaved
29 as noisy detectors reporting perception in trials where no light was sent. DN
30 subjects were significantly faster to take decisions. Reaction times significantly
31 increased with the decrease in the number of photons. This trend was reflected in
32 the latency and onset of the EEG responses over frontal and parietal contacts
33 where the first significant differences in latency comparable to differences in
34 reaction time appeared. Delays in latency of neural responses across intensities
35 were observed later over visual areas suggesting that they are due to the time
36 required to reach the decision threshold in decision areas rather than to longer
37 integration times at sensory areas. Our results suggest that post-retinal processing
38 significantly contribute to increase detection noise and thresholds, decreasing the
39 efficiency of the retina brain detector system.

40

Introduction

41

42 The first experiments on the sensibility of the human eye to weak, near absolute
43 thresholds, optical signals were conducted in the 1940s (Hecht, 1942). They led to the
44 conclusion that rod photoreceptors can detect a very small number of photons, typically
45 less than 10 during an integration time of about 300 ms (Barlow, 1956). This prediction
46 has been confirmed by several experiments (Rieke and Baylor, 1998) making from the
47 human eye a remarkable light sensitive detector, which can easily stand a comparison to
48 today's best man-made detectors (Rieke and Baylor, 1998). This has even led to the
49 proposal of using the human eye as a detector for quantum phenomena such as
50 entanglement (Brunner, 2008; Sekatski et al., 2009).

51 The quantum efficiency (QE) of the human eye as a detector, i.e., the probability
52 of getting a response given that a photon impinges on the retina, has been determined into
53 two different ways: behaviorally and by direct neural recordings. In behavioral terms the
54 QE can be estimated from the frequency of seeing curves (Foes) (Hecht, 1942) later
55 replaced by a distribution of ratings (Sakitt, 1972) . Flashes of light, with a controlled
56 probabilistic distribution of photons are sent into the pupil and subjects who are dark
57 adapted are prompted to indicate if they perceived a flash. The detection threshold, i.e.,
58 the number of photons required to trigger a conscious percept (arbitrarily defined as the
59 light intensity giving rise to 60% detection), is determined by measuring the fraction of
60 trials in which a flash is reported as perceived as a function of the number of photons
61 incident at the cornea. Since, only about 8% of the photons incident on the cornea reach
62 the retina, hence about 100 photons are required to trigger a neural response even if rod
63 photoreceptors can react to single photons (Rieke and Baylor, 1998).

64 Direct neural recordings have been used in toads (Baylor, 1979) and monkeys
65 (Baylor, 1984) to determine QE from the number of photons needed to evoke responses
66 in isolated rod photoreceptors. These studies lead to the conclusion that rod
67 photoreceptors can signal the absorption of single photons. Consequently, estimates of
68 QE vary in about one order of magnitude as a function of the definition of response
69 (neural response in photoreceptors vs. behavioural responses) used for its quantification.
70 Behavioural measurements based on the FoS curve place the quantum efficiency (QE) of
71 the human eye between 0.03 and 0.06 while direct estimates based on losses within the
72 eye range from 0.1 to 0.3 (Baylor, 1979). Consequently, the QE estimated from
73 behaviour is very low compared with the absorptive QE estimated from the properties of
74 light photoreceptors at the retina.

75 The reasons for the divergence in the estimated and measured QE are not
76 completely clear as the processes limiting sensitivity are not yet fully characterized.
77 When estimating QE from the FoS curve we demand to the observer to indicate whether
78 or not they perceived the stimuli. According to classical psychophysical models (Krantz,
79 1969), this detection process is composed of at least two psychological components or
80 processes: 1) the sensory process transforming the physical stimulation into internal
81 sensations and 2) a decision process which decides on responses based on the output of
82 the sensory process. Each of the two processes (see Figure 1) is, in turn, characterized by
83 at least one parameter: The sensory process by a sensitivity parameter and the decision

84 process by a response criterion parameter. To avoid confounding the sensitivity of the
85 sensory process with the response criterion of the decision process, one needs to measure
86 two aspects of detection performance: the conditional probability that the observer says
87 “yes” when a stimulus is present (the hit rate, or True positive rate closely linked to the
88 FoS curve) but also the conditional probability that the observer says “yes” when the
89 stimulus is not present (False positive rate or FAR).

90 Barlow (Barlow, 1956;Hallett, 1969) relied on the concept of false positive
91 responses to explain the discrepancy in QE. He attributed the fact that observers
92 occasionally report seeing a flash even when no light was delivered to the existence of
93 what he termed “dark light” or “dark noise”. Behavioural sensitivity and dark noise can
94 be the result of Poisson fluctuations in photon absorption at the level of the retina.
95 Experiments in toads have shown that one of the possible source of this dark-noise is the
96 thermal ionization of the photosensitive protein in the retina, pointing that sensitivity of
97 frog was decreasing with temperature (Aho et al., 1993). Upon this model, dark noise
98 increases the rate of false-positive affecting the sensitivity of the detection threshold and
99 the reliability of the QE estimated from behavior.

100 Is retinal noise the only factor impacting the response criterion that characterizes
101 the decision process? If this were the case then retinal (dark) noise would be the only
102 explanation for the observed discrepancy in QE. Yet, noise is not an exclusive property of
103 retinal photoreceptors. Noise might arise anywhere into the chain of neural processing
104 and add to fluctuations at the level of the retina. Supporting the existence of postretinal
105 contributions to dark noise are the multiple experiments that rely on Transcranial
106 Magnetic Stimulation (references) at the level of the occipital cortex to evoke
107 phosphenes. Some of these studies indicate that the phosphene perception appears after
108 extensive recurrent processing and is therefore not purely attributable to primary visual
109 processing (Taylor et al., 2010). In addition, deciding that the stimulus is present or
110 absent is clearly not a matter of sensory evidence alone as a decision about stimulus
111 absence lacks sensory evidence by definition. Interestingly, cells coding for the decision
112 about both, the absence and presence of stimulus, have been recently reported at the
113 prefrontal cortex of primates (Merten and Nieder, 2012). Noise at the level of prefrontal
114 cells might equally impact decisions contributing to the discrepancy in QE. The impact of
115 post-retinal processing on the reduction of QE remains unknown.

116 To shed further light on the post-retinal mechanisms impacting the quantum
117 efficiency of the human eye we repeated a version of the FoS experiment described in
118 (Hecht, 1942). We hypothesized that post-retinal processes substantially contribute to the
119 observed decrease in QE when inferred from the FoS curve. We adhered to the only
120 accessible measure of QE we can rigorously control in this experiment, i.e., the fraction
121 of incident photons that contribute to conscious perception as measured by the FoS curve.
122 Besides psychophysics and signal detection theory, we relied on two other
123 complementary methodologies helpful to dissociate the stages of processing impacting
124 sensitivity (see Figure 1). First, reaction times (mental chronometry) which allows
125 inferring to some extent the content, duration, and temporal sequencing of cognitive
126 operations within perceptual processes (Jensen, 2006). Second, scalp measured Event
127 related Potentials (ERPs) which provide an indicator of the latency of neural responses at
128 the different processing stages (Thorpe et al., 1996).

129

130 **Material and Methods**

131 **1. Recording Protocol**

132 *Participants*

133 Twelve healthy young volunteers (age range: 26-38, mean age 30 ± 4 , 2 females)
134 were recruited from the faculties of Physics and Medicine of the University of Geneva.
135 Eleven of the participants were right-handed. They had no history of neurological
136 problems. The whole experiment was approved by the local ethics committee (Geneva
137 University Hospitals). Participants were verbally informed of the goals of the experiment
138 and the sequence of events.

139 *Dark adaptation*

140 The experiment was carried out in a completely dark recording room with all
141 potential sources of light, e.g., computer LEDs, covered by black plastic tape.
142 Participants were dark-adapted before the experiment by being kept during 40 minutes in
143 the dark room while wearing a black sleeping mask. The darkness was kept during the
144 approximately two hour's duration of the experiment.

145 *Rationale of the experiment and instructions to participants*

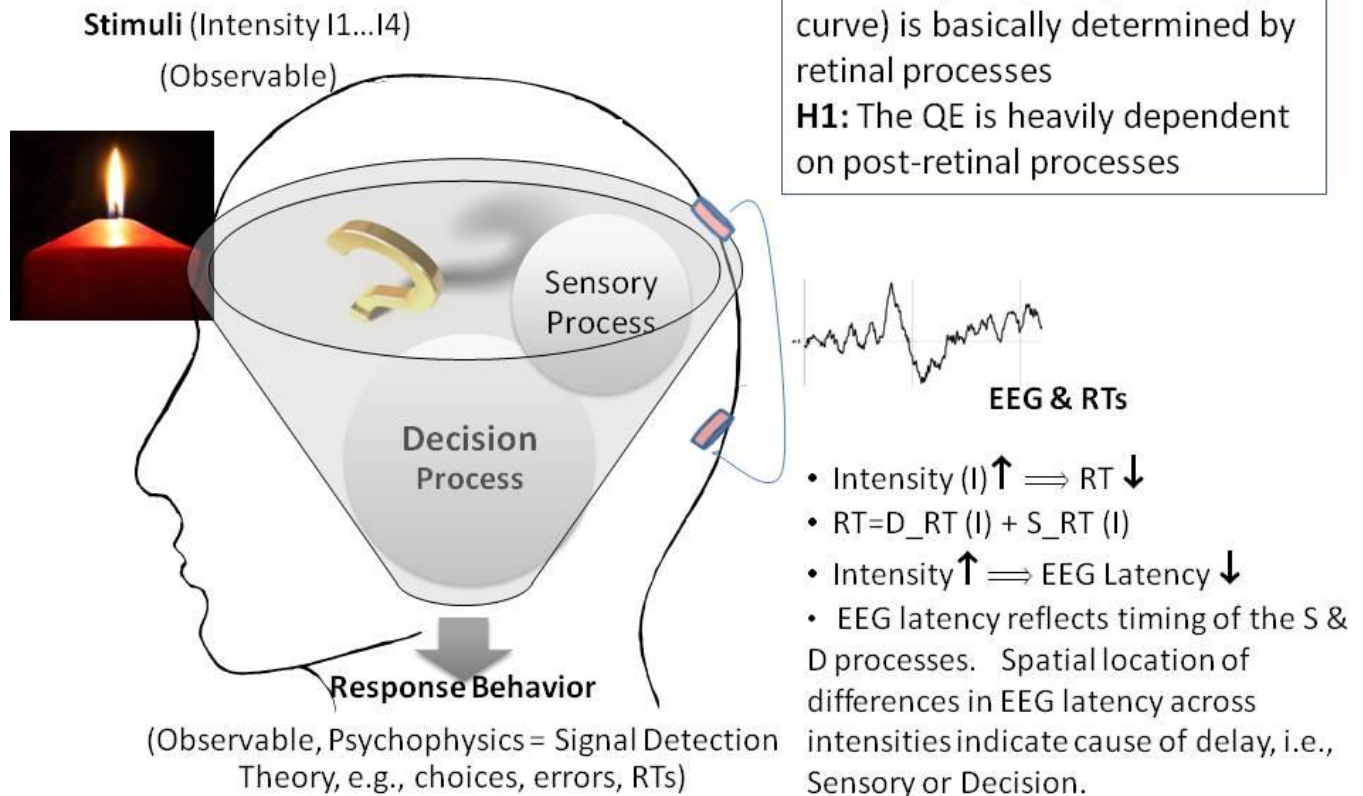
146 As illustrated in Figure 1, we don't have direct access to the sensory and decision
147 processes we would like to disentangle in this study. We therefore need to infer the
148 contribution of each process through the analysis of observable measures of neural activity
149 such as the EEG or from behavior (using for example Signal detection theory and RTs).
150 We expected increases in sensitivity but decreases in RTs with stimulus intensity. While
151 sensitivity is generally a relatively stable property of the sensory process across subjects,
152 the decision criterion can vary widely from subject to subject and from time to time. We
153 then expected to capture information about the interindividual variability and sources of
154 noise linked to decisions through the investigation of reaction times. By combining
155 information from reaction times and the latency and scalp positions of peaks in the ERP
156 signal we expected to extract information on the relative timing of the sensory and
157 decision processes. According to current decision making models, decisions are taken
158 when sufficient evidence in favor of one of another choice has been accumulated.
159 Decisions occur when neural signals reach a certain threshold. Noise alters the gradual
160 accumulation of neural information speeding up or retarding the decision time.
161 Consequently, one should expect that differences in peak latencies which correlate with
162 differences in RTs across stimulus intensities appear above the areas where neural
163 responses are being accumulated. Depending on whether the differences appear over
164 sensory or decision areas one can then infer the timing of their relative contributions.

165 The link between the FoS and RTs can be expressed as:

$$FoS = f(I) \leftrightarrow I = f^{-1}(FoS)$$
$$RT = g(I) \leftrightarrow RT = g(f^{-1}(FoS)) = h(FoS)$$

166 where I is the number of photons sent. According to this expression, the RT is 1) a
167 function of the frequency of seeing (FoS) and 2) dependent on the decision process.

sensory process (S): Transforms physical stimulation into internal sensations
decision process (D): Decides on responses based on the output of the sensory process



168
 169
 170

Figure 1

171 The instruction given to the subjects was explicit: “report seeing the flash via a button
 172 press when you feel completely confident about the percept”. We avoided a multiple
 173 choices task reflecting the trial by trial confidence in perception (Barlow, 1956) & Sakitt
 174 (Sakitt, 1972). We did so on three bases: 1) Reaction Times are known to vary as a
 175 function of the difficulty of the task. Yet, the difficulty of the task is not only linked to
 176 the perceptual difficulty that we want to investigate here but also to the number of
 177 choices available. There is ample experimental evidence supporting the increase in
 178 reaction times with the number of available choices. Since we were interested in the link
 179 between perceptual processes and reaction times rather than on the link between choices
 180 and reaction times we considered the two choices alternative as the most reasonable one.
 181 2) The number of errors is known to increase with number of choices as repeatedly
 182 shown in the literature. This is sometimes due to false button presses. Since choosing
 183 between several buttons in full darkness is more challenging than under normal
 184 illumination conditions then the probability of false button presses increases.
 185 Consequently, the two choices task adopted here is “optimal” to: (i) isolate real “dark

186 noise” coming from retinal/post-retinal effects from motor mistakes and (ii) to isolate the
187 perceptual component of the reaction times from the choice component. 3) Subject’s
188 performance and EEG signals tend both to worsen with the duration of the experiments.
189 As previously explained, multiple choices tasks lengthen the experiment. A condition for
190 the experiment is to remain attentive and still as to obtain adequate signal to noise ratios
191 in EEG signals and sustained performance. This posed a challenge to some of the
192 participants as the full experiment lasted for approximately 2.30 hours.

193

194 *EEG Recordings*

195 The scalp electroencephalogram (EEG, 64 channels) and reaction times (RTs)
196 were recorded during the experiment. The EEG was recorded at variable frequency
197 sampling (1024 Hz or 2048Hz) to guarantee the temporal precision of the triggers and
198 response time. Frequency sampling was individually selected on the basis of the initial
199 psychometric curves. Recordings were done using the Biosemi system with 64 sintered
200 Ag-AgCl electrodes and implicit filter settings at 5th order sinc filter with a -3 dB point at
201 1/5th of the sampling frequency. The electrodes were mounted on the manufacturer-
202 provided cap according to an extended 10-20 system. The Biosemi system uses a
203 common mode sense (CMS) active electrode as the reference. Visual inspection was used
204 to reject artifact-contaminated trials. Bad electrodes interpolation was based on spherical
205 splines using Cartool. Epochs of 1100 ms (100 ms before the presentation of the
206 stimulus) were extracted after notch filtering at 50 Hz and superior harmonics. Baseline
207 correction was based on 100ms prestimulus window.

208 *Experimental Setup*

209 The experimental design is schematically depicted in Figure 2. A light emitting
210 diode (LED) was used to produce flashes of light at 500nm wavelength which guarantees
211 maximum sensitivity of rod cells (Alpern, 1987). A portion of the light was collimated
212 and coupled into a single mode fiber. This kind of optical source was chosen for safety
213 reasons as only a maximum power of hundreds of pW can be coupled into the fiber. The
214 LED was software controlled via a National Instruments digital to analog card that allows
215 varying the power of each light pulse between 8 pW and 400 pW, while its duration can
216 be chosen between 100 μ s and 1ms. In this way, the number of photons in each pulse can
217 be dynamically varied by nearly three orders of magnitude. We used neutral density
218 filters (grey filters) to further decrease the optical intensities by a factor t_{ND} and adapt
219 them to the subject’s sensitivity that was individually detected as described in next
220 section. While t_{ND} changes from subject to subject it is set to at least 0.1.

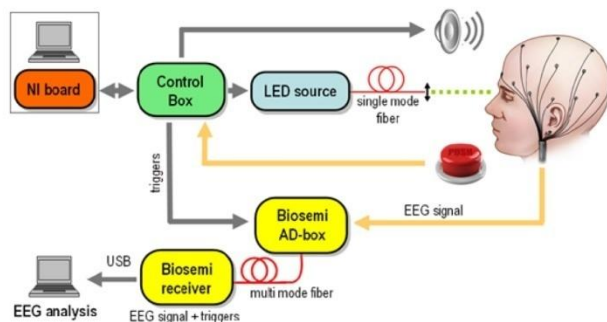


Figure 2

221

222 The light coupled into the fiber was directed to one eye of the subject, who rested
223 his chin and forehead on a chinrest support to keep the head steady over the experiment.
224 A collimation lens at the end of the fiber allows focusing of the beam on the retina. Since
225 the density of rod cells (the most sensitive human photo-receptors) is highest in the
226 peripheral region of the retina, the direction of the beam is chosen to form an angle of
227 approximately 20 degrees with respect to the eye's axis. The retina is illuminated on the
228 temporal side, to avoid the optical nerve. At least 700 ms before the light is emitted, an
229 acoustic signal is produced to alert the subjects of the imminent emission of the pulses.
230 The subjects press a button in case of conscious perception of the flash and a digital
231 signal is sent to the NI board. The communication with the board is managed via a
232 control box. Finally, the control box sends to the Biosemi AD-Box the trigger signals
233 corresponding to 1) the timing of the acoustic signal, 2) the value of the randomly chosen
234 intensity and 3) the timing of the button press for perceived flashes. At least 150
235 repetitions of each intensity and the same amount of blank trials (the acoustic signal is
236 given but the flash is not sent) were obtained per each subject. The time course of the
237 whole experiment is shown in Figure 3.

238

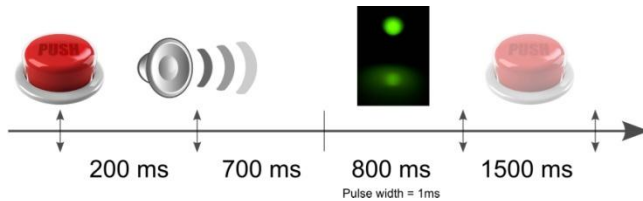


Figure 3

239

240 *Estimating the Number of photons incident at the cornea as a function of the*
241 *power emitted by the LED.*

242 The power emitted by a LED is linear with respect to the voltage bias applied to it
243 and linearity was assessed in our case to hold up to 9 Volts. A calibrated power meter
244 was used to measure the power P which exits the fiber. The number of photons per
245 second corresponding to the power measured when the LED is at 9V is given by:

$$246 \quad n^* = \frac{P\lambda}{hc} \quad (1)$$

247 where λ is the wavelength, h is Planck constant and c is the speed of the light. For each
248 subject 4 different intensities were individually selected by varying the voltage applied to
249 the LED from the $V_{offset} \approx 2.5 V$ to $9 V$. As the power emitted by the LED is linear
250 between 2.5V and 9V, the value of P in equation (1) must be multiplied by a factor
251 $t_{bias} = (V_I - V_{offset}) / (9V - V_{offset})$, where V_I the voltage is applied to the LED for the
252 specific intensity I .

253 The fact that the grey filters reduce the power by a factor t_{ND} must be taken into
254 account into the calculations as well as the fact that the pulses had a very short duration
255 Δt_{pulse} that varied according to the subject from 0.5 to 1 ms. Therefore, the final formula

256 used to compute the number of photons at each pulse that were sent to the cornea is
257 finally given by:

$$258 \quad n_{pulse} = \frac{t_{bias} \times t_{ND} \times \Delta t_{pulse} \times P \times \lambda}{h \times c} \quad (2)$$

259

260 *Selection of the best individual parameters (Method of Adjustment)*

261 Once subjects were adapted to darkness and the EEG set up installed we carried
262 out some initial tests to individually tune the attenuation of light (achieved by the grey
263 filters) and the duration of the pulses. Several attenuations were tested for each of the
264 four intensities and subjects were requested to report if they perceived the flashes. The
265 final attenuations were chosen as those for which the flashes were perceived in half of the
266 presented pulses. This approach was preferred to the on-line selection of the intensities in
267 order to minimize the duration of the experiment. Finally, during the experiment, four
268 intensities of flashes were presented to each subject with attenuations chosen to evoke
269 perception in half of the trials. From now on, we will use the term intensity for the
270 intensity of the beam reaching the cornea, i.e., after the filters.

271

272 **2. Data analysis and rationale**

273 *2.1 Reaction Time Analysis*

274 We investigated if and how reaction times, defined as the time elapsed between
275 the onset of the flash and the button press indicating perception, vary as a function of 1)
276 the number of incident photons, and 2) the accuracy of decisions. There is indeed
277 growing evidence from primate neurophysiology indicating that in reaction time tasks, a
278 perceptual choice is made when the firing rate of a selective cortical neural population
279 reaches a threshold (Lo and Wang, 2006). Reaction times (RTs) therefore correlate with
280 the time needed to reach the threshold that is dependent on the difficulty of the choice
281 (Smith, 2004). Weak or uncertain stimuli lead to slowly varying accumulation of
282 evidence and longer decision times while certain/strong stimuli lead to quickly growing
283 accumulation of certitude that is reflected in a sharp build up of neural activity that
284 quickly reaches the necessary threshold to reach decisions speeding up the reaction times.
285 On this basis we should expect: 1) an inverse dependency between reaction times and the
286 intensity (number of photons) of the flashes, 2) Significant differences between mean
287 RTs corresponding to different stimulus intensities. On the other hand, subjects
288 performing a visual detection task need to manage the tradeoff between speed and
289 accuracy (Ratcliff, 2002).

290

291 *2.2 Statistical analysis of Behavioral data*

292 RTs were compared using the one-way ANOVA if data had a normal distribution
293 (according to the Lilliefors test, matlab statistical toolbox, 0.05 significance level) or
294 using the Kruskal-Wallis test (nonparametric one-way ANOVA) for non-normally
295 distributed data. Unless otherwise specified, all the statistics and analysis were done
296 using Matlab R2006a. When appropriated, we display behavioral data using notched

297 boxplots that provide a summary of several important features of the distribution of
 298 values (e.g., median, confidence interval around it, outliers). In these plots, when the
 299 notches of two or more groups do not overlap then the medians of the two groups differ
 300 at the 5% significance level.

301

302 *2.3 Frequency of Seeing (Accuracy) and QE*

303 The 4 pre-selected intensities and the blank trials were presented to the subjects in
 304 random order with each intensity repeated at least 150 times. The frequency of seeing
 305 curve was obtained plotting the proportion of flashes reported as perceived as a function
 306 of the intensity. The energy of the flashes was transformed into the average number of
 307 photons using equation (2).

308 The probability of seeing decrease with the decrease in the number of presented
 309 photons. However, determining which threshold should be used to determine the minimal
 310 number of photons necessary to generate conscious detection is still an open question.
 311 Hecht & al set the threshold at 60% of probability and concluded that 54 to 148 incident
 312 photons are needed to trigger conscious detection. Here, we decided to set a slightly
 313 lower threshold at 50%. This is due to three reasons, 1) we introduced under the form of
 314 zero intensity trials a control against dark noise, i.e., detection by chance and 2) we used
 315 several naïve (untrained) subjects and 3) the experimental design introduced a variable
 316 delay between the acoustic signal and the photons arrival to prevent anticipation.

317 In order to more precisely estimate the number of flashes absorbed by the retina
 318 that are necessary for conscious perception from discrete observations, the probability of
 319 seen curve is typically fitted with a model. For instance, Rieke (Rieke and Baylor, 1998),
 320 following Hecht (Hecht, 1942), made the assumption that for a given intensity the
 321 number of photons absorbed by the retina follows a Poisson-distribution. In Rieke's
 322 model, the probability of seeing a flash (p_{see}) of intensity I can be written as:

$$323 \quad p_{see}(I) = \sum_{n=\theta}^{\infty} \frac{e^{-\alpha I}}{n!} (\alpha I)^n \quad (3)$$

324 Where θ is the minimal number of photons, under which the subject never perceived a
 325 flash and α represents the decrease in intensity between the number of photon sent in the
 326 flash and the amount of photons arriving at the retina. The value $\alpha \times I$ represents thus the
 327 mean number of photon absorbed by the retina.

328 However, after extensive testing on the data we found that much better fits are
 329 obtained assuming a log-poisson regression model distribution, i.e.,

$$330 \quad p_{see}(I) = \sum_{n=\theta}^{\infty} \frac{e^{-\log(\alpha I)}}{n!} \log(\alpha I)^n \quad (4)$$

331 The free parameters θ and α were therefore determined by the simultaneous
 332 minimization of the objective function f given by:

$$333 \quad f(\theta, \alpha) = \sum_{k=1}^4 \left[p_{see}(I_k) - \sum_{n=\theta}^{\infty} \frac{e^{-\log(\alpha I_k)}}{n!} \log(\alpha I_k)^n \right]^2 \quad (5)$$

334 Where I_k are the four intensities presented to each subject. Note that the fits are here
 335 used to get an adequate approximation of the number of photons needed for conscious

336 detection at the 50% probability. By no way, should these fits be considered as a model
337 for the detection probability as they have been obtained from just four intensities.

338

339 *2.5 Measuring sensitivity using signal detection theory: the sensitivity index (d')*
340 *and the Receiver Operating Curve (ROC)*

341 A criticism to the FoS curve as a measure of sensory sensitivity is that it mixes the
342 decision criteria with sensory sensitivity. We therefore used as an additional measure the
343 sensitivity index (d') which splits detection performance into two components: the
344 conditional probability that the observer says “yes” when a light is present (the hit rate or
345 true positive rate TPR) and the conditional probability that the observer says “yes” when
346 a light is not present (the false alarm rate, or false positive rate FN) (Green and Swets,
347 1966). We computed the sensitivity index d' as:

$$d' = z(FPR) - z(TPR)$$

348 where $z(\cdot)$ denotes the z-score of the given probabilities, FPR is the false-positive rate
349 and TPR is the true-positive rate. Since $z(0) = \infty$, we replaced FPR by $1/N$, with N
350 denoting the number of trials, for subjects showing perfect specificity.

351 A different way to test the overall efficiency of the human visual system is to use
352 the ROC curve, a measure coming from signal detection theory (Fawcett, 2006). The
353 ROC curve is the plot of the fraction of true positives (i.e. true positive rate TPR) vs. the
354 fraction of false positives (i.e. false positive rate FPR) of a binary classifier as its
355 discrimination threshold is varied. A true positive (TP) is a non-zero intensity trial
356 reported as perceived while a true negative (TN) is a non perceived zero intensity trial. A
357 false negative (FN) is a non zero intensity trial that is non perceived and a false positive
358 is a zero intensity trial reported as perceived. The TPR and FPR are respectively defined
359 as:

360 $TPR = TP/(TP + FN)$ (6)

361

362 $FPR = FP/(FP + TN)$ (7)

363 The advantage of the ROC over the FoS is that it allows quantifying both, the sensitivity
364 of the observer given by the TPR as well as his/her specificity defined as $1-FPR$.

365

366 *2.7 EEG analysis*

367 ERPs were computed by averaging the epochs reported as perceived by button
368 presses, once aligned by the flash onset for every subject and intensity. Both, the original
369 Biosemi reference and the average reference were used in the analysis to assess
370 independence of the effects on the chosen reference. Note that the average reference
371 removes the effect of a constant from the data. The Grand Mean (GM) was afterwards
372 computed as the average over subjects of the individual ERPs once normalized by the
373 norm of the global scalp energy. This normalization avoids overweighting the
374 contribution of individual subjects to the GM.

375 The excellent (millisecond basis) resolution of the EEG makes it suitable to
376 investigate the timing and scalp topography of the neural responses as a function of the
377 variations in the number of perceived photons. The timing of the responses might help to
378 elucidate post-retinal contributions to the QE of the visual system. Indeed, it has been
379 observed that neural activity needs to reach a certain decisional threshold before the
380 stimuli is perceived. Weak stimuli lead to builds up in neural activity characterized by
381 flatter slopes than strong stimuli. Therefore, we should expect that the timing of the
382 component of the ERPs varies as a function of the stimulus intensities over areas
383 involved in perceptual or decisional processes. In fact, if perceptual decisions are
384 responsible for the QE of the visual system, delays in the ERPs as a function of the
385 intensity should already appear at the level of the primary visual cortex reflecting the
386 transmission delays at the retinal level. On the other hand, if there are post-retinal
387 contributions to the QE, we should expect additional delays over frontal or parietal areas
388 known to be involved in decisional processes. Consequently, the analysis of ERPs might
389 help us to elucidate the contribution of the different brain regions to the dependency of
390 the reaction times with intensity. Indeed, if delays already occur in the transmission of
391 signals from the retina, delays (differences in the latency of the ERP components) in the
392 ERPs at the level of the primary visual cortex should be observed. On the other hand, if
393 decisional processes are the only responsible for the delays in the behavioral responses,
394 the first delay observed should appear on ERPs of brain areas involved in more complex
395 and cognitive processes, as parietal and prefrontal areas

396 To evaluate the delays in the mean ERPs responses (as well as for the Grand
397 Mean ERPs) as a function of the intensity we computed for each participant and for each
398 electrode, the pair-wise time-lagged Spearman's rank correlations (Wilcoxon and Muska,
399 2001) between the different intensities on overlapping temporal windows of 100 ms
400 duration. Because noise in the recordings could have blurred the results, windows with
401 irrelevant signal-to-noise ratio ($SNR < 3$) were not considered. The SNR was defined for
402 each temporal window as the ratio between the mean of the signal power and its variance.
403 The power rather than the raw signal was used in the definition to avoid negative voltage
404 values. The analysis window covered the 1100 milliseconds period following stimulus
405 onset. The delay for each 100 ms window and for each electrode was selected as the one
406 for which the maximum significant ($p < 0.01$) correlation was obtained. To obtain
407 summary values across subjects we computed the Fisher transform of the correlations and
408 then averaged out over subjects. Note that while the Fisher transformation can fail to
409 provide the correct statistics when the correlations are computed using the Pearson's
410 correlation it is as accurate as bootstrap when more robust non parametric measures of
411 correlations such as the Spearman's rank are used. The significance of the correlation R
412 at the individual means and GM levels was computed in Matlab by transforming the
413 correlation into a t statistic having $n-2$ degrees of freedom, where n is the number of time
414 points in the analysis window, i.e. ≈ 100 (*from* : $(100 - \text{time lag}) \times 1024 / 1000$).
415 The confidence bounds are based on an asymptotic normal distribution of $1/2 \times$
416 $\ln(1 + R/1 - R)$, with an approximate variance equal to $1/(n - 3)$ (Press, 1989). We
417 corrected the p -value with the product of the number of electrodes (64)
418 and the number of time windows (55). This analysis was done using the original Biosemi
419 reference placed over the occipital cortex and repeated using the average reference to
420 make sure that results were reference independent.

421

422

Results

423

424

Dark Noise concerns half of the investigated population

425

426

427

428

429

430

431

432

433

434

435

436

437

438

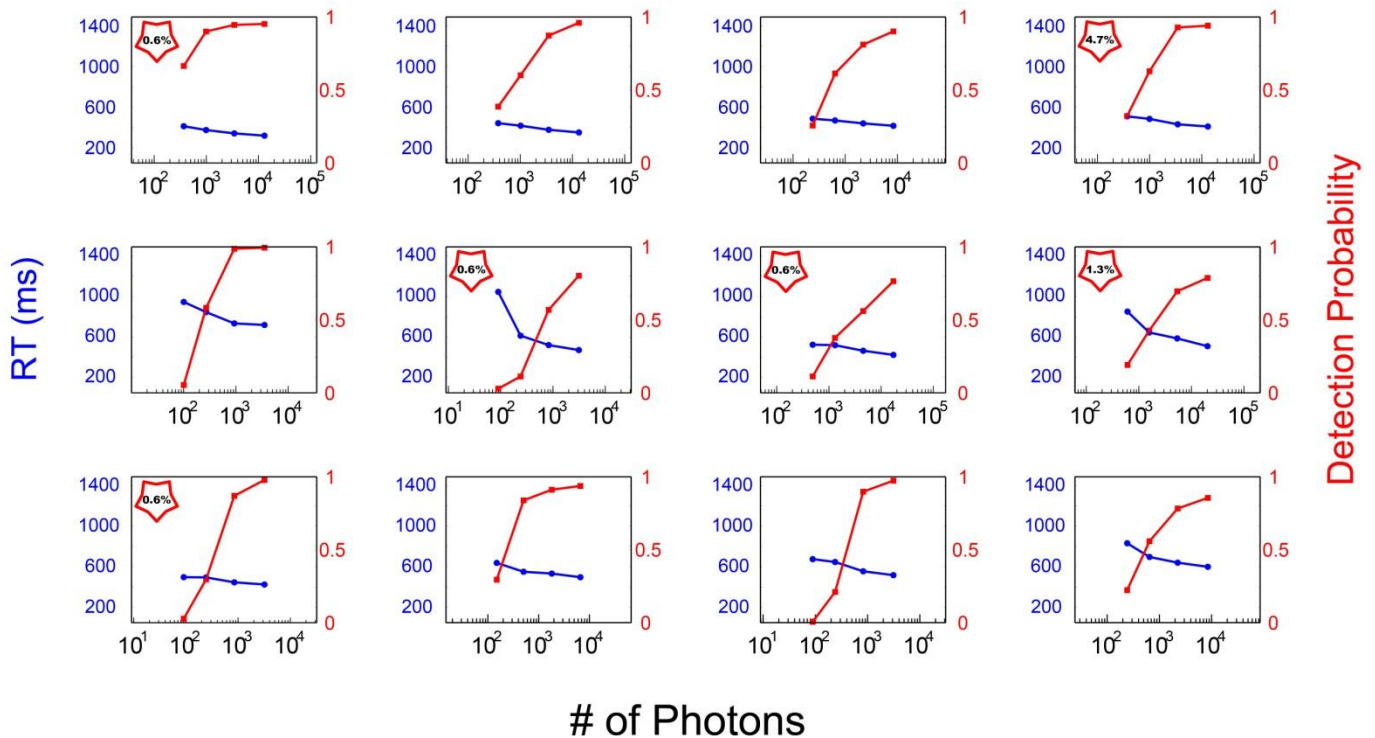


Figure 4

439

440 As can be seen from Figure 4, exactly half of the participants in the experiment
441 reported seeing flashes when no light was emitted, while the other half showed no
442 evidence of dark noise. Consequently, on the basis of the reduced sample of subjects
443 considered here (N=12), we have to conclude that the probability of observing Dark
444 Noise in a population of young healthy controls is exactly 0.5 and therefore significantly
445 different from zero (binomial test, $p=0$). This criterion allows for a natural splitting of
446 the subjects according to behavior. However, it is likely that all subjects might exhibit
447 Dark noise if the number of trials increases.

448

449 *Frequency of Seeing (Accuracy) and QE*

450 The estimated number of incident photons necessary to elicit conscious perception
451 determined from the log-Poisson fits to the frequency of seeing curve considerably varied
452 across participants (mean: 815, min 181, max: 3051, std: 903) for a threshold set at 50%.
453 Once these values were corrected by the 0.08 factor estimated by Hecht we obtained:
454 mean: 65, min 17, max: 244, std: 72. The last subject, requiring 244 photons, reported
455 considerable visual fatigue during the experiment. In addition, we observe a non-
456 significant ($p=0.11$, t-test, $p=0.12$, ranksum test) but noticeable trend for better
457 performance in young volunteers used to work in the darkness with respect to naïve
458 subjects. This observation, that requires further experimental research, suggests that the
459 efficiency in the conscious detection of dim light might be improved by practice as seen
460 in previous experiment (Hecht, 1942; Sakitt, 1972). This would be hardly the case if
461 visual performances were exclusively dependent on retinal contributions.

462 *Sensitivity Index (d')*

463 Contrarily to the FoS curve which basically reflects the hit rates, the sensitivity
464 index also contemplates the false alarms. Note that the d' index depicted in Figure 5b
465 shows a dependency with the number of incident photons similar to the one in the FoS
466 curve (Figure 5a). This measure allows moreover distinguishing the poorer performances
467 of the noisy subjects.

468

469 *DN subjects have smaller sensitivity to specificity ratios (area under the ROC*
470 *curve) than NDN subjects while sensitivity is similar.*

471 Both, the mean and the median area under the ROC curve were significantly
 472 lower ($p = 0.0191$, parametric t-test on the mean and $p = 0.0022$, ranksum non-parametric
 473 test on the median) for the group of DN subjects (mean = 0.67 ± 0.05 , DN; mean = $0.74 \pm$
 474 0.01 , NDN; median = 0.69 , DN; median = 0.75 , NDN) than for the NDN subjects.
 475 However, no significant differences ($p > 0.05$ in both cases) between groups were
 476 detected on the mean or median true positive rates suggesting that sensitivity is identical
 477 in both groups (DN mean = 0.3345 , NDN mean = 0.3652 , DN median = 0.39 , NDN
 478 median = 0.4294). Differences in the area under the ROC curve, a composed measure of
 479 the trade-off between specificity and sensitivity, indicate that DN subjects are more prone
 480 to report false percepts but they are as accurate as non dark noise subjects in detecting

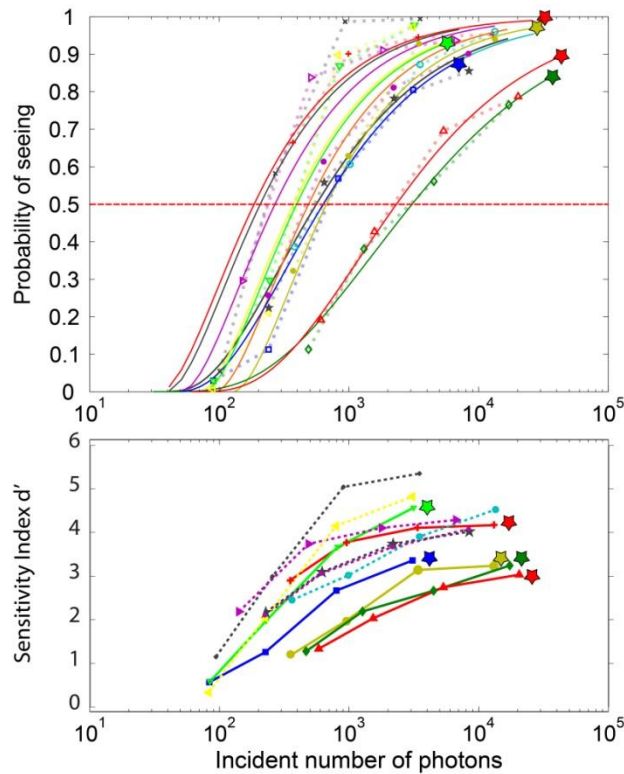


Figure 5

481 similar number of photons. This observation is supported by the statistical comparison of
 482 both groups in terms of the number of photons required to elicit conscious perception at
 483 50% of the trials as detected from the FoS curve. Indeed, assuming that only 8% of the
 484 emitted photons reach the retina we see that DN subjects require on mean 54 photons to
 485 elicit perception in 50% of the trials while noiseless subjects require around 35 photons
 486 on mean with no significant differences between groups detected by a parametric (t-test,
 487 $p = 0.14$) or a non-parametric test (rank sum, $p = 0.33$).

488

489 *DN subjects are significantly faster to take decisions than noiseless subjects.*

490 As argued before, in perceptual choice tasks as the one here, experimental
 491 evidence indicate that choices are made when the firing rate of selective cortical neural
 492 population reach a threshold. Reaction times (RTs) therefore correlate with the time

493 needed to reach the threshold that is dependent on the difficulty of the choice. This effect
 494 was clearly observed in our data. The plot of RTs as a function of the intensity of the
 495 flashes showed a clear decrease in RTs for increasing intensities at both, the individual
 496 (Figure 4) and population level (Figure 6).

497 As shown in Table 1, the comparison between the distribution of reaction times
 498 between subjects with and without dark noise revealed significant differences for all the
 499 analyzed intensities. DN subjects were significantly faster to take decisions than NDN
 500 subjects. Differences between groups were considerable and varied from 58 ms for the
 501 lowest intensity to 100 ms or more for all the others. The rank sum test, as any non-
 502 parametric method, is robust to skewed distributions as it makes no assumption about the
 503 underlying distribution. In addition, the Lillietest revealed no significant deviations in
 504 this dataset from the normality assumption indicating that our RT distributions were not
 505 skewed.

506

507 **Table 1: Comparison of mean reaction times between DN and NDN subjects. Statistical analyses**
 508 **were performed using parametric (t-test) or non-parametric tests (rank sum). P-values lower than**
 509 **10^{-6} are marked as 0.**

Intensity	Mean RT DN	Mean RT NDN	Pval (parametric test, t-test)	Pval parametric rank sum)	(non test,
I1	587	645	0.03	0	
I2	502	621	0	0	
I3	474	573	0	0	
I4	437	541	0	0	

510

511

512

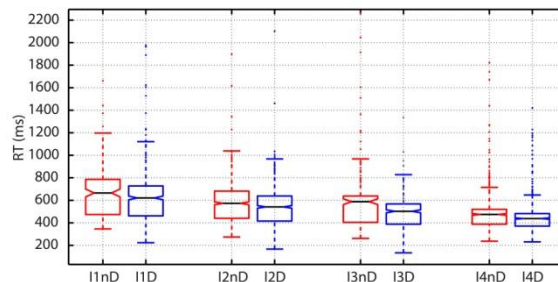


Figure 6

513

514

515 *EEG Results*

516 The grand mean ERPs for the four different intensities are shown in Figure 7.
517 From the figure, it can be readily seen that the early ERP components (N70 and P100)
518 characteristic of visual ERPs in the presence of visible stimuli are absent over contacts
519 placed over primary visual areas, e.g., electrodes Iz and Oz. Moreover, the first
520 significant ($p < 0.01$) deviations in the GM amplitude with respect to a baseline period of
521 200ms (z-scores ≥ 2.5 standard deviations away from the baseline mean) were observed
522 first at frontal (Fpz, 211 ms for the strongest intensity), and slightly later for Occipital
523 electrodes (Iz, Oz, 251 ms for the strongest intensity).

524 The onset, latency and amplitude of the first ERP component recorded over frontal
525 electrodes varied gradually as a function of the intensity of the stimulus. The
526 stronger stimuli (black trace) peaked first than the other intensities. The delay across
527 intensities was more clearly observed on the second, negative ERP component peaking
528 between 400 and 600 ms and appeared over frontal, parietal and occipital electrodes.

529

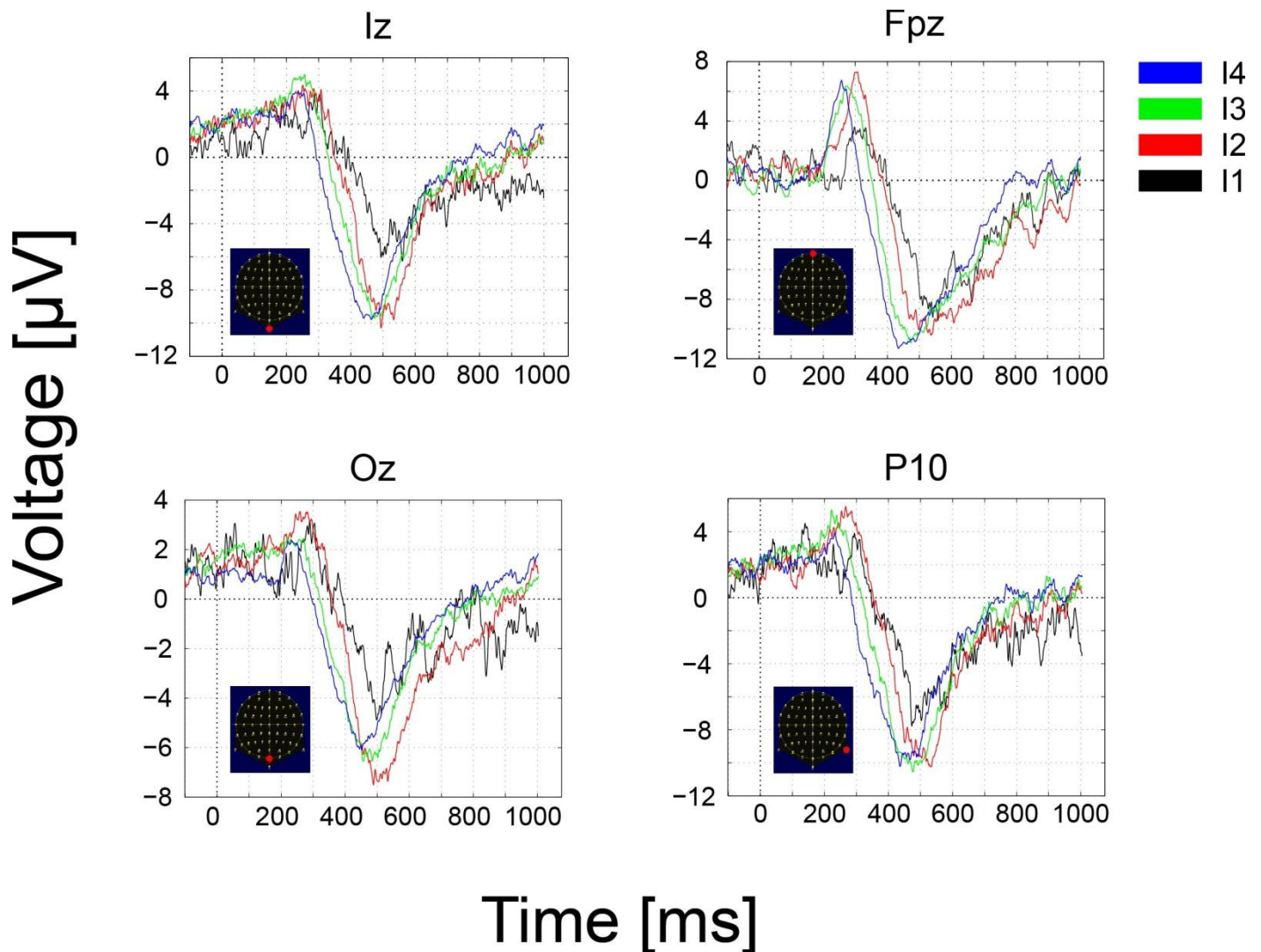
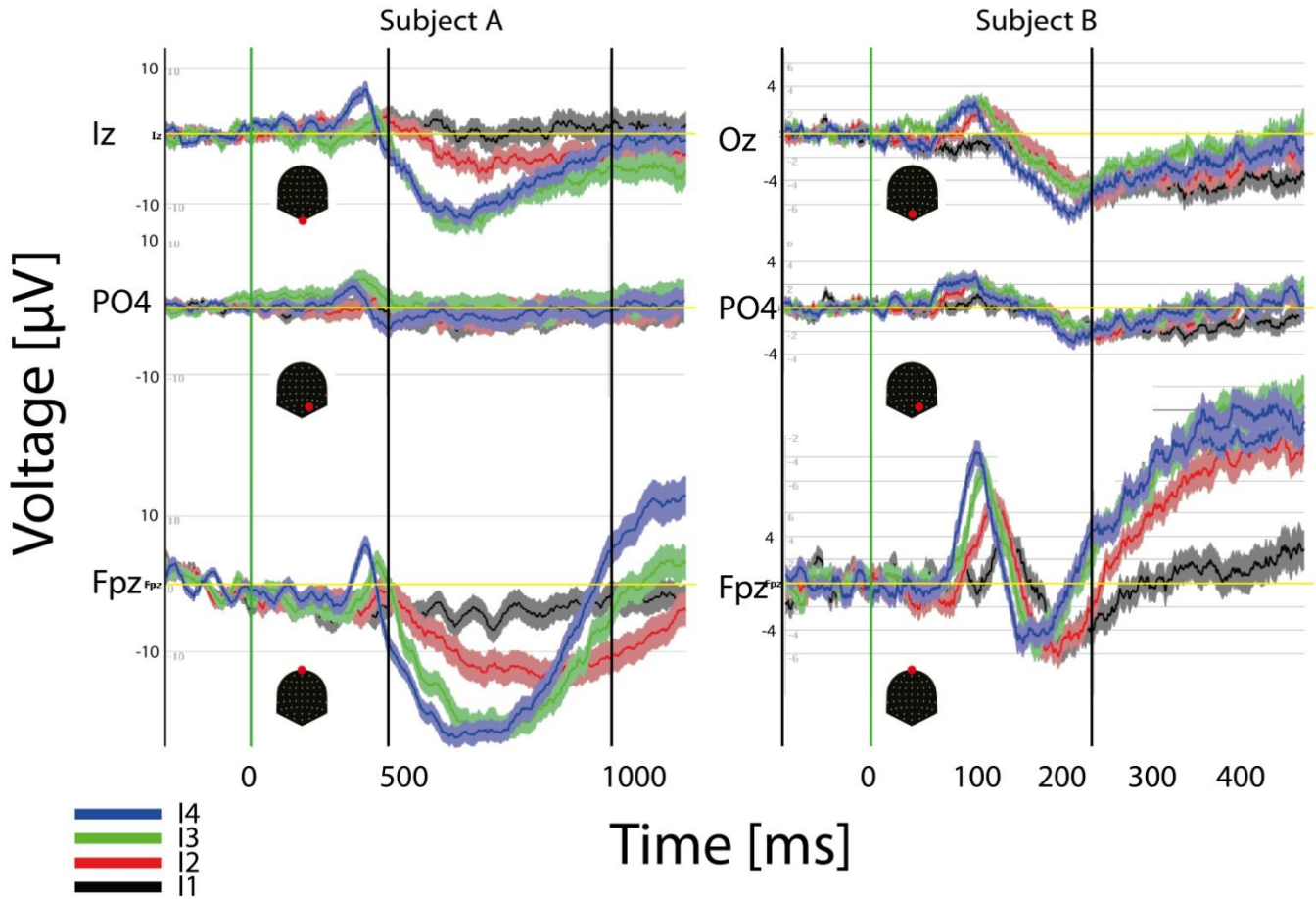


Figure 7



531

Figure 8

532

533

534

535

536

537

538

539

540

541

542

543

544

545

546

547

548

549

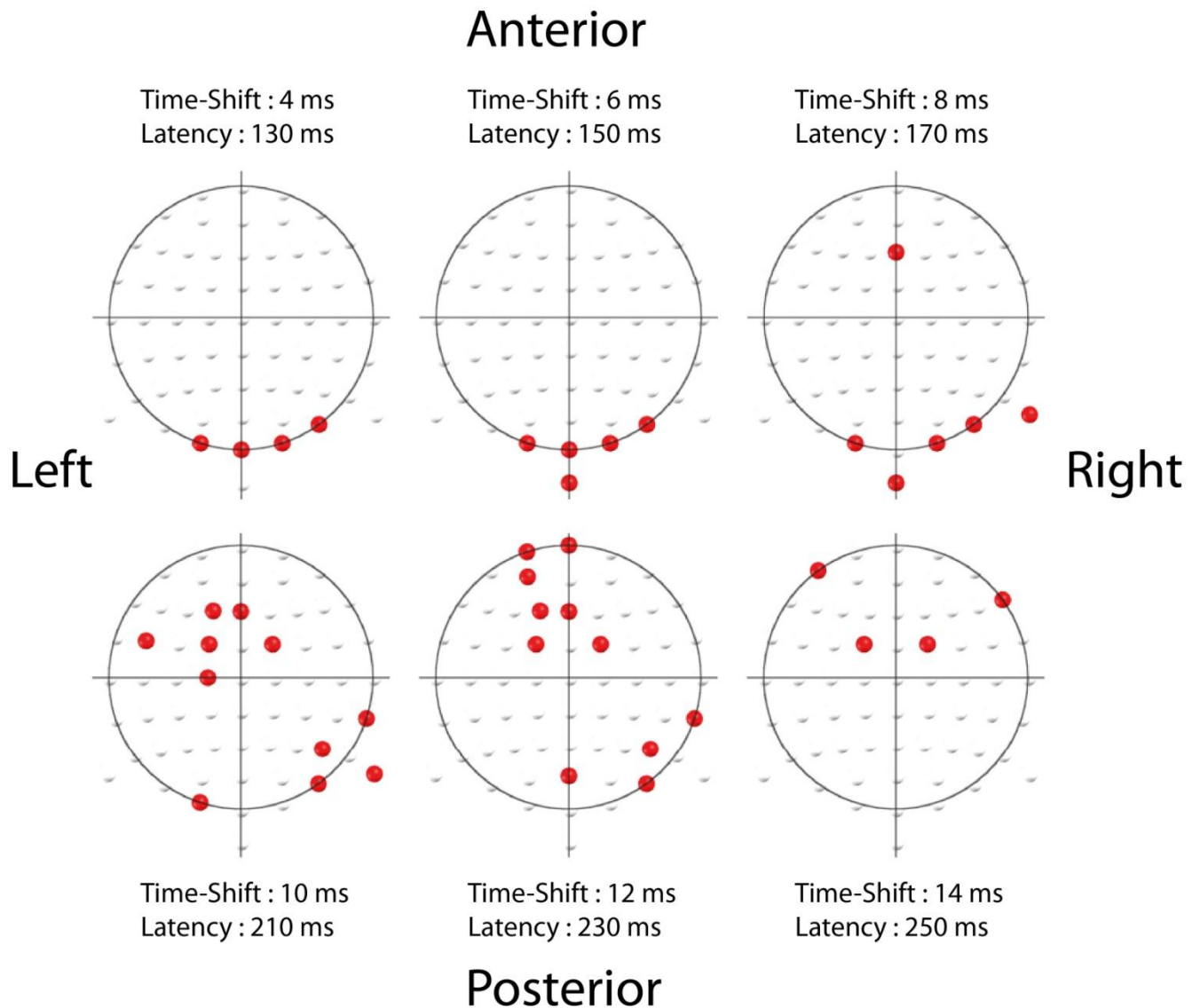
ERP results at the single subject level are illustrated in Figure 8. In this case the ERP for the four different intensities (dark thick traces) and the standard error around the mean are depicted for three channels and two different subjects. Each subject is shown in a different column. As observed for the Grand Mean data peak delays across intensities are obvious over frontal contacts (FPz) and much smaller or inexistent over parietal and occipital contacts. Polarities and latencies of the components are similar to those observed for the GM data. Note that occipital responses for the lowest intensity (black trace) are absent at the initial processing stages suggesting that a critical mass of activation of the primary visual cortex necessary to produce the ERP components is absent.

The results of the analysis of the Grand-Mean ERP suggest that the observed behavioral delays in processing the weaker stimuli are mostly introduced by fronto-parietal areas. This observation would be in agreement with the idea that differences in reaction times are due to accumulative effects that involve both retinal and post retinal stages. Our observation is not compatible with decision delays being caused by only longer integration times at the level of the retina. If this were indeed the case the delays should appear at electrodes over visual areas at least as early as in frontal areas. The

550 Grand Mean ERP results therefore suggest that decisional processes play a major role in
551 slowing down responses to weak or faint visual stimuli as suggested by the animal
552 literature. Nevertheless, the analysis of the GM data obscures the contribution of
553 individual subjects and is certainly sensitive to the variability in reaction times observed
554 across subjects. Moreover, this simple ERP analysis is likely to miss latency differences
555 between small ERP components from early visual areas as it has been observed that the
556 intensity of early visual responses in primates V1 decreases with the contrast of the
557 stimuli although the latency of responses increases (Chen et al., 2008).

558

559



560

561 **Figure 9**

562

563 To obtain summary statistics over subjects while accounting for interindividual
564 variability we relied on the cross-correlation analysis described at the end of the methods
565 section. In this analysis the goal is to investigate at the individual level, the electrodes
566 showing significant delays in neural responses and to obtain summary statistics once the
567 inter individual differences are accounted for. This method has the advantage of
568 highlighting potentially significant correlations between weak signals that might be
569 overlooked with the more traditional approach based on Grand Mean ERP. The statistical
570 results for this analysis are shown in Figure 9. In the picture, electrodes showing the
571 earliest significant correlation ($r > 0.6$, $p\text{-value} < 0.005$) for a given temporal shift (delay)
572 between two intensities (I4 and I3) are indicated by red dots.

573

574 As seen from the picture, the electrodes showing the earliest significant
575 correlation between the two higher intensities I3 and I4 vary as a function of the time
576 delay tested. For short temporal delays, signal shifts of approximately 5ms the more
577 significant correlations appear over occipital electrodes. When the time shifts increase to
578 ~10-20 ms, the more significant correlations progressively shift to frontal electrodes. The
579 latency at which electrodes show the earliest significant correlation also covariates with
580 the shift in the signals. For instance, the earliest significant correlation detected across
581 intensities changes from 130 ms for shifts of 4ms to 250 ms for the 14ms delay.
582 Importantly, in the analysis described here we exclusively reported the electrodes for
583 which the earliest significant differences are seen to minimize the potential influence of
584 feedback information (top-down) from high level visual areas into primary visual areas
585 (Bullier, 2001) While not shown here, we observed that delays of approximately 15 ms
586 first seen in parietal areas were later observed in visual areas. The results of the cross-
587 correlation analysis can be then summarized as follow: Small but significant delays of
588 approximately 5 ms across intensities are initially seen over occipital electrodes. Delays
589 become longer (~14ms) and shift to middle central and then to frontal areas when we
590 approach the response times. Consequently, the results are more compatible with a non-
591 linear accumulation of delays across the different processing stages - from perception to
592 decisions - than with a pure retinally induced delay.

593

594 While from the scalp topography it is impossible to infer the precise localization
595 of the generators of delays, the very small yet early delays observed over occipital
596 contacts such as Iz, Oz, O1 and O2 (systematically linked to the earliest visual responses)
597 are insufficient to explain the much longer differences in RTs of about 30ms observed for
598 example between intensities I3 and I4. The small early differences in visual areas confirm
599 that a component in RT variability is due to longer integration times at the level of the
600 retina and primary visual areas as already suggested by previous studies ((Pins and
601 Bonnet, 1996;Chen et al., 2008)) and phenomena like the Pulfrich and Hess effects.
602 However, our results strongly suggest that frontal and parietal networks, traditionally
603 linked in invasive studies to decision making processes, are much more involved in the
604 variability of the response times. Noteworthy, while visual responses are hard to evoke
605 and measure using the scalp EEG for such small number of photons, we believe that the
606 results of the analysis described here, and in particular the early detection of the small
607 shifts over occipital electrodes corroborates the sensitivity of our approach to weak
608 signals. Indeed, our results are consistent with animal data which suggest that: 1) neural

609 responses in the lower order neurons are too reliable to account for variability in decision
610 time (Schall, 2002) and 2) neural responses in primates from ganglion cells (Croner et al.,
611 1993 ;Sun et al., 2004) to V1 in alert monkeys (Gur et al., 1997;Gur and Snodderly,
612 2006) are highly stereotyped in response times. Consequently, animal and human data
613 agree to pinpoint cortically mediated post sensory processing as the major source of
614 variance in RT (Cao and Pokorny, 2010).

615
616

617

618 **Discussion**

619

620 In this study, we investigated the quantum efficiency (QE) of the human visual
621 system to further clarify: 1) the sources affecting the QE, 2) the divergence between
622 experimental (in animal) and behavioral (in humans) estimates of QE, 3) the origin
623 (retinal or post-retinal) of processes limiting behavioral sensitivity such as the so-called
624 “dark noise”, i.e., observers who occasionally report seeing a flash even when none is
625 delivered.

626 The QE can be estimated from the frequency of seeing curves (FoS) following
627 Hallet (1969). Flashes of light, with a controlled probabilistic distribution of photons
628 were sent into the pupil of 12 dark-adapted subjects who were prompted to indicate if
629 they perceived or not a light. EEG and reaction times were measured along the
630 experiment. The detection threshold, i.e., the number of photons required to trigger a
631 conscious percept, was determined by measuring the fraction of trials in which a flash
632 was reported as perceived as a function of the number of photons incident at the cornea.
633 Despite considerable interindividual variability, we concluded that on mean around 70
634 photons are required for untrained subjects to trigger perception 50% of the time even
635 though photoreceptors can react to single photons.

636 Therefore, in agreement with previous experiments the QE estimated from
637 behavior is very low compared with the absorptive QE estimated from the properties of
638 light photoreceptors at the retina. Either much more photons are required to elicit
639 conscious perception than to elicit responses in photoreceptors or dark noise increases the
640 rate of false-positive affecting the sensitivity of the detection threshold and the reliability
641 of the behavioral QE.

642 The use of behavioural and neurophysiological measures added to the FoS curve
643 allowed to shed further light on the origins of the dark noise. Indeed, exactly half of the
644 subjects showed this effect indicating that behavioral sensitivity considerably varies
645 across individuals. As argued in (Rieke and Baylor, 1998) the dark noise might be the
646 consequence of Poisson fluctuations in photon absorption at the level of the retina.
647 Indeed, continuous noise in mammalian rods can generate fluctuations that look very
648 much like true photon responses (Baylor, 1984). If Poisson fluctuations were generating
649 the dark noise one would expect randomly generated action potentials (APs) at the level
650 of the retina that are transferred to the cortex generating the false percept. Moreover, the
651 generation of each AP is independent of all the other spikes as noise is not expected to

652 simultaneously arise in all retinal cells simultaneously. In this case spikes would be
653 completely described by a random Poisson process. This would imply that all subjects
654 should exhibit the same probability of randomly generated action potentials during the
655 experiment.

656 However, in a Poisson process the probability of observing random spikes, which
657 could be interpreted as false percepts, increases with the length of the interval, i.e. with
658 the time between the stimuli onset and the decision. It is therefore surprising that DN
659 subjects are significantly faster when in fact; if dark noise were the consequence of
660 Poisson fluctuations at the level of the retina we should expect the converse effect.

661 Nonlinearities at the retinal level can clearly contribute to the discrepancy
662 between physical QE and perceptual QE. While we cannot fully justify our answer with
663 the available data we believe that retinal nonlinearities alone cannot fully explain the
664 observed differences. Indeed, the trial by trial variability within the same observer for
665 identical number of photons is hard to explain on purely retinal basis. As the physical
666 parameters of the stimuli and that of the cornea are invariant across trials the only
667 possible alternative left is that thermal noise is leading to the trial by trial variability. Yet,
668 the influence of thermal noise seems to be reduced when the number of photons is
669 increased as detection becomes much more accurate.

670 An alternative is to consider that a significant amount of noise is introduced post-
671 retinal photoreceptor. For instance, dark noise, or at least part of it, could arise during the
672 neural decision making process and as the result of speeded decisions. Indeed, our results
673 fit better to this hypothesis. According to current decision models in cortical areas (Gold
674 and Shadlen, 2007), the accuracy of decisions is inversely proportional to decision time.
675 Yet, given the low false-positive rate of DN subjects ($< 5\%$), it would be unlikely that
676 dark-noise events leading to true positive detection could have significantly decreased the
677 mean reaction time of DN subjects (see Figure 6).

678 There is growing evidence from primate neurophysiology indicating that in
679 reaction time tasks, a perceptual choice is made when the firing rate of a selective cortical
680 neural population reaches a threshold (Lo and Wang, 2006). Reaction times (RTs)
681 therefore correlate with the time needed to reach the threshold that is dependent on the
682 difficulty of the choice (Smith, 2004). Weak or uncertain stimuli lead to slowly varying
683 accumulation of evidence and longer decision times while certain/strong stimuli lead to
684 quickly growing accumulation of certitude that is reflected in a sharp build up of neural
685 activity that quickly reaches the necessary threshold to reach decisions speeding up the
686 reaction times. It has been also suggested that the threshold can be tuned to optimize the
687 trade-off between speed and accuracy (Smith, 2004).

688 The fact that there are no differences in sensitivity between both groups of
689 subjects combined with the significantly shorter RTs for the DN individuals is compatible
690 with post-retinal contributions to the decision processes according to current models. This
691 view is supported by the well known perception of phosphenes, i.e. false percepts of light
692 or Dark Noise, after Transcranial Magnetic Stimulation over the occipital cortex.
693 Interestingly, conscious phosphene perception does not appear to be a phenomenon local
694 to the occipital cortex but rather a consequence of extensive recurrent processing (Taylor
695 et al., 2010). Existing experimental evidence therefore suggest that noise leading to false

696 percepts might arise at the level of the visual cortex, extrastriate cortex or be induced at
697 any later decisional stage that provides feedback to primary visual areas. Consequently,
698 dark noise does not appear to be purely driven by retinal contributions.

699 The analysis of the EEG recordings additionally suggests that post-retinal
700 contributions play a major role in the decrease in sensitivity measured from the FoS
701 curves. First, the size of the neural signals over primary visual areas was practically zero
702 for the lowest intensity suggesting that a critical mass of neural activation was not
703 reached in the early processing stages. Second, delays in neural responses as a function of
704 the intensity of the stimuli – comparable with behavioral delays – were found at
705 electrodes clustered around frontal and fronto-central regions that have been traditionally
706 linked to decision making. This result coincides with animal electrophysiology
707 suggesting that perceptual choices are driven by the activity of selective cortical
708 population in decision areas.

709 There are several limiting aspects in this study. First, we are lacking a thorough
710 estimation of the psychometric functions since only four intensities were tested per
711 subject. Yet, increasing the number of intensities per subject would have lead to a hardly
712 tolerable duration for the experiment impacting the reliability of the EEG signals and the
713 behavioral responses. Second, we were not able to achieve a reasonable number of false
714 alarms at the individual level as to build a robust mean ERP for these events. While the
715 number of trials is largely sufficient for robust ERPs for hit trials this is not the case for
716 the false alarms that amount to a few trials in just half of the sampled population. We
717 were therefore unable to investigate in more detail the neural origin of these events.
718 Third, we did not measure RTs for the missed trials. This decision was taken because
719 RTs and false alarms are known to increase with the number of choices available to the
720 participant. However, the nature of false alarms is different in latest case as they are often
721 due to mistakes in button presses. This is a serious concern when working in full
722 darkness. Therefore, in order to identify false alarms strictly linked to false percepts we
723 preferred to keep the choices to a minimum which certainly renders many interesting
724 analysis impossible.

725

726 In summary, our results are consistent with a major contribution of post-retinal
727 processing to the QE when measured in terms of the FoS curve. In support of this idea,
728 we observed 1) an inverse dependency between reaction times and the intensity (number
729 of incident photons), 2) Significant differences between mean RTs corresponding to
730 different stimulus intensities for all subjects, 3) Significant differences in RTs between
731 DN and NDN subjects with DN subjects being significantly faster, 4) delays in perceptual
732 decisions are explained by delays in mean ERP responses localized to fronto-central areas
733 rather than primary visual areas. The fact that delays are explained by fronto-parietal
734 areas, known to be involved in decision making reinforce the idea of post-retinal
735 contribution to deficits in sensitivity. Our results are then compatible with Piéron's law
736 that states that, at a constant intensity of the background, reaction times are inversely
737 proportional to the intensity of the target stimulus and independent of the sensorial
738 system (Piéron 1913; Pins and Bonnet 2000). They are also in agreement with the early
739 visual processing described in (Pins and Bonnet, 1996) and results from invasive
740 recordings (Bell et al., 2006) showing that increasing visual stimulus intensity reduces the

741 onset latency of visual responses in several areas outside the primary visual system such
742 as the superior colliculus.

743

744 The main conclusion of this study is then that the absorptive QE estimated from
745 the properties of light photoreceptors at the retina is pretty accurate and the human eye is
746 one of the best existing light detectors. However, the QE estimated from behavior is very
747 low as the detector is composed from two different sensors: the retina and the brain. The
748 brain adds a large contribution to the decrease in sensitivity and the losses in QE of the
749 whole system. Low evidence thresholds seem to appear in some subjects that reach faster
750 decisions to the expenses of perceptual errors such as dark noise. In summary, the FoS
751 curves considerably underestimate the QE of the human eye due to post-retinal neural
752 noise that add to fluctuations at the level of the retina.

753

754

755

References

- 756
757
758
759
760
761
762
763 Aho, A.C., Donner, K., and Reuter, T. (1993). Retinal origins of the temperature
764 effect on absolute visual sensitivity in frogs. *The Journal of Physiology*
765 463, 501-521.
- 766 Alpern, M. (1987). A note on the action spectrum of human rod vision. *Vision*
767 *Res.* 27, 1471-1414.
- 768 Barlow, H.B. (1956). Retinal noise and absolute threshold. *J Opt Soc Am* 46,
769 634-639.
- 770 Baylor, D., Lamb, Td, Yau, Kw (1979). Responses of retinal rods to single
771 photons. *J Physiol.* 288, 613-634.
- 772 Baylor, D.A., Nunn, B., Schnapf, J.L. (1984). The photocurrent, noise and
773 spectral sensitivity of rods of the monkey *Macaca fascicularis*. *J. Physiol.*
774 357, 575-607.
- 775 Bell, A., Meredith, M., Van Opstal, A., and Munoz, D. (2006). Stimulus intensity
776 modifies saccadic reaction time and visual response latency in the
777 superior colliculus. *Experimental Brain Research* 174, 53-59.
- 778 Brunner, N., Branciard, C., Gisin, N. (2008). Can one see entanglement ? *Phys.*
779 *Rev. A* 78.
- 780 Bullier, J. (2001). Integrated model of visual processing. *Brain Research Reviews*
781 36, 96-107.
- 782 Cao, D., and Pokorny, J. (2010). Rod and cone contrast gains derived from
783 reaction time distribution modeling 10.1167/10.2.11 *Journal of Vision* 10
- 784 Chen, Y., Geisler, W.S., and Seidemann, E. (2008). Optimal temporal decoding
785 of neural population responses in a reaction-time visual detection task.
786 *Journal of Neurophysiology* 99, 1366-1379.
- 787 Croner, L.J., Purpura, K., and Kaplan, E. (1993). Response variability in retinal
788 ganglion cells of primates *Proceedings of the National Academy of*
789 *Sciences of the United States of America* 90 8128-8130
- 790 Fawcett, T. (2006). An introduction to ROC analysis. *Pattern Recognition Letters*
791 27, 861-874.
- 792 Gold, J.I., and Shadlen, M.N. (2007). The neural basis of decision making.
793 *Neuroscience* 30, 535.
- 794 Green, D.M., and Swets, J.A. (1966). *Signal detection theory and psychophysics*.
795 Wiley New York.
- 796 Gur, M., Beylin, A., and Snodderly, D.M. (1997). Response Variability of Neurons
797 in Primary Visual Cortex (V1) of Alert Monkeys. *J. Neurosci.* 17, 2914-
798 2920.
- 799 Gur, M., and Snodderly, D.M. (2006). High Response Reliability of Neurons in
800 Primary Visual Cortex (V1) of Alert, Trained Monkeys
801 10.1093/cercor/bhj032. *Cerebral Cortex* 16, 888-895.

802 Hallett, P.E. (1969). Quantum efficiency and false positive rate. *J Physiol.* 202,
803 421–436.

804 Hecht, S., S. Schlaer, and H.P. Pirenne. (1942). Energy, quanta and vision. *J.*
805 *Gen. Physiol.* 25, 819-840.

806 Jensen, A.R. (2006). *Clocking the mind: Mental chronometry and individual*
807 *differences*. Amsterdam: Elsevier.

808 Krantz, D.H. (1969). Threshold theories of signal detection. *Psychological*
809 *Review* 76, 308.

810 Lo, C.-C., and Wang, X.-J. (2006). Cortico-basal ganglia circuit mechanism for a
811 decision threshold in reaction time tasks. 9, 956-963.

812 Merten, K., and Nieder, A. (2012). Active encoding of decisions about stimulus
813 absence in primate prefrontal cortex neurons. *Proceedings of the National*
814 *Academy of Sciences* 109, 6289-6294.

815 Pins, D., and Bonnet, C. (1996). On the relation between stimulus intensity and
816 processing time: Piéron's law and choice reaction time. *Attention,*
817 *Perception, & Psychophysics* 58, 390-400.

818 Press, W.H., Flannery, B. P., Teukolsvky, S.A., Vetterling, W.T., (1989).
819 *Numerical Recipes in Pascal*. Cambridge: Cambridge University Press.

820 Ratcliff, R. (2002). A diffusion model account of response time and accuracy in a
821 brightness discrimination task: fitting real data and failing to fit fake but
822 plausible data. *Psychon Bull Rev* 9, 278-291.

823 Rieke, F., and Baylor, D.A. (1998). Single-photon detection by rod cells of the
824 retina. *Reviews of Modern Physics* 70, 1027 LP - 1036.

825 Sakitt, B. (1972). Counting every quantum. *The Journal of Physiology* 223, 131-
826 150.

827 Schall, J.D. (2002). Decision Making: Neural Correlates of Response Time.
828 *Current biology : CB* 12, R800-R801.

829 Sekatski, P., Brunner, N., Branciard, C., Gisin, N., and Simon, C. (2009).
830 Towards Quantum Experiments with Human Eyes as Detectors Based on
831 Cloning via Stimulated Emission. *Physical Review Letters* 103, 113601.

832 Smith, P.L., Ratcliff, R. (2004). Psychology and neurobiology of simple decisions.
833 *TRENDS in Neurosciences* 27, 161-168.

834 Sun, H., Rüttiger, L., and Lee, B.B. (2004). The spatiotemporal precision of
835 ganglion cell signals: a comparison of physiological and psychophysical
836 performance with moving gratings. *Vision Research* 44, 19-33.

837 Taylor, P.C.J., Walsh, V., and Eimer, M. (2010). The neural signature of
838 phosphene perception. *Human Brain Mapping* 31, 1408-1417.

839 Thorpe, S., Fize, D., and Marlot, C. (1996). Speed of processing in the human
840 visual system. 381, 520-522.

841 Wilcox, R.R., and Muska, J. (2001). Inferences about correlations when there is
842 heteroscedasticity. *British Journal of Mathematical and Statistical*
843 *Psychology* 54, 39-47.

844

845

846

847 **Figure and table legends**

848

849 **Figure 1: Rationale of the experiment and main hypothesis.**

850

851 **Figure 2: Experimental Setup.** A light emitting diode (LED) was digitally controlled to
852 produce pulses of light at 500nm wavelength with power varying between 8 pW and 400
853 pW and very short duration (between 100 and 1ms depending on the subject). The power
854 of the light was individually adjusted to each participant using grey filters and sent through
855 collimation lens at the end of the fiber to optimally focus the beam to form an angle of
856 approximately 20 degrees with respect to the eye's axis retina where the density of rods is
857 higher. EEG recordings, done using the Biosemi system, were synchronized with the
858 beams onset at the μ s level. Around 180 repetitions of four different intensities of light
859 were randomly presented to each participant. In addition an equivalent number of trials
860 (180) were included where participants received a warning signal but no light beam was
861 actually sent into the retina.

862

863 **Figure 3: Schematic illustration of the timing of the experiment.** The light pulses were
864 equally randomly distributed within a time window of 800 ms after the auditory signal.
865 The subjects had 1500 ms to indicate by a button press if they perceived or not the flash.

866

867 **Figure 4: Psychometric curves (red) and reaction times (blue) of each subject.**

868 Individual RTs and frequency of seeing curves as a function of the number of
869 photons in the light beam (abscissa). The left and right ordinates depict the RTs and
870 the proportion of perceived flashes respectively. No point is depicted in the graph if
871 the number of flashes reported by the subject as perceived is identically zero when
872 no flash was sent. DN subjects are signaled with a red star, which contains the false-
873 positive rate.

874

875 **Figure 5: Top: Psychometric curve for each subject.** The symbols represent actual
876 data, while the plain lines are their respective log-poisson fits. Each subject is
877 represented in a different color. These fits are used to estimate the minimal number of
878 incident photons required to elicit perception in at least 50% of the trials. The log-
879 poisson distribution allows a reasonable fit for all subjects, even if for a few subjects a
880 linear Poisson distribution may lead to a better fit. The bigger stars at the top of the
881 curves indicate subjects with non-zero false-positive rate. **Lower inset: d-prime**
882 **sensitivity index for each subject.** DN Subjects with non-zero false-positive rate
883 (plain lines) have a lower d-prime than the NDN subjects.

884

885 **Figure 6: Variations in reaction time (RT) as a function of the intensity of the beam**
886 **when subjects are divided into two groups according to the presence (DN) or absence**
887 **(NDN) of false detection (dark noise).** The red bars represent the 95% confidence
888 interval. DN = Dark-Noise (Grey), NDN = Non-Dark Noise (White).

889

890 **Figure 7: Grand-Mean ERPs over occipital (Iz, Oz), middle frontal (FPz) and**
891 **parietal contacts (P10) as a function of the intensity of the beam (the four effective**

892 light intensities). Responses are ordered from the strongest to the weakest intensity (I1 to
893 I4) and the following color convention is used: I4, black; I3, red, I2, green, I1, blue. Note
894 that the onset, latency and amplitude of the first ERP component recorded over frontal
895 electrodes varies as a function of the intensity of the stimulus, i.e., the stronger intensity
896 in black peaks earlier than the other intensities. Delays in neural responses across
897 intensities occur earlier over frontal, and parietal electrodes. The strongest intensities (I4,
898 black) lead to the fastest response and the weakest (I1, blue) to the slowest.

899

900 **Figure 8: Individual (2 subjects) ERP averages** for the four intensities at occipital,
901 parietal and frontal electrodes. The highest intensities show faster response at the three
902 sites but effects are more pronounced over frontal contacts.

903

904 **Figure 9: Correlation-Based Analysis of intensity-dependant ERP delays :** Schematic
905 top view of the electrodes (black) showing first, among electrodes at a given latency and
906 for given temporal shift, significant correlation (> 0.6), p-value (< 0.005) and SNR (> 3)
907 between intensities 3 and 4.